

Net charge fluctuations in Au + Au collisions at $\sqrt{s_{NN}} = 130$ GeV

J. Adams,³ C. Adler,¹² M. M. Aggarwal,²⁵ Z. Ahammed,²⁸ J. Amonett,¹⁷ B. D. Anderson,¹⁷ M. Anderson,⁵ D. Arkhipkin,¹¹ G. S. Averichev,¹⁰ S. K. Badyal,¹⁶ J. Balewski,¹³ O. Barannikova,^{28,10} L. S. Barnby,¹⁷ J. Baudot,¹⁵ S. Bekele,²⁴ V. V. Belaga,¹⁰ R. Bellwied,⁴¹ J. Berger,¹² B. I. Bezverkhnay,⁴³ S. Bhardwaj,²⁹ P. Bhaskar,³⁸ A. K. Bhati,²⁵ H. Bichsel,⁴⁰ A. Billmeier,⁴¹ L. C. Bland,² C. O. Blyth,³ B. E. Bonner,³⁰ M. Botje,²³ A. Boucham,³⁴ A. Brandin,²¹ A. Bravar,² R. V. Cadman,² X. Z. Cai,³³ H. Caines,⁴³ M. Calderón de la Barca Sánchez,² A. Cardenas,²⁸ J. Carroll,¹⁸ J. Castillo,¹⁸ M. Castro,⁴¹ D. Cebra,⁵ P. Chaloupka,⁹ S. Chattopadhyay,³⁸ H. F. Chen,³² Y. Chen,⁶ S. P. Chernenko,¹⁰ M. Cherney,⁸ A. Chikanian,⁴³ B. Choi,³⁶ W. Christie,² J. P. Coffin,¹⁵ T. M. Cormier,⁴¹ J. G. Cramer,⁴⁰ H. J. Crawford,⁴ D. Das,³⁸ S. Das,³⁸ A. A. Derevschikov,²⁷ L. Didenko,² T. Dietel,¹² X. Dong,^{32,18} J. E. Draper,⁵ F. Du,⁴³ A. K. Dubey,¹⁴ V. B. Dunin,¹⁰ J. C. Dunlop,² M. R. Dutta Majumdar,³⁸ V. Eckardt,¹⁹ L. G. Efimov,¹⁰ V. Emelianov,²¹ J. Engelage,⁴ G. Eppley,³⁰ B. Erazmus,³⁴ P. Fachini,² V. Faine,² J. Faivre,¹⁵ R. Fatemi,¹³ K. Filimonov,¹⁸ P. Filip,⁹ E. Finch,⁴³ Y. Fisyak,² D. Flierl,¹² K. J. Foley,² J. Fu,⁴² C. A. Gagliardi,³⁵ M. S. Ganti,³⁸ T. D. Gutierrez,⁵ N. Gagunashvili,¹⁰ J. Gans,⁴³ L. Gaudichet,³⁴ M. Germain,¹⁵ F. Geurts,³⁰ V. Ghazikhanian,⁶ P. Ghosh,³⁸ J. E. Gonzalez,⁶ O. Grachov,⁴¹ V. Grigoriev,²¹ S. Gronstal,⁸ D. Grosnick,³⁷ M. Guedon,¹⁵ S. M. Guertin,⁶ A. Gupta,¹⁶ E. Gushin,²¹ T. J. Hallman,² D. Hardtke,¹⁸ J. W. Harris,⁴³ M. Heinz,⁴³ T. W. Henry,³⁵ S. Heppelmann,²⁶ T. Herston,²⁸ B. Hippolyte,⁴³ A. Hirsch,²⁸ E. Hjort,¹⁸ G. W. Hoffmann,³⁶ M. Horsley,⁴³ H. Z. Huang,⁶ S. L. Huang,³² T. J. Humanic,²⁴ G. Igo,⁶ A. Ishihara,³⁶ P. Jacobs,¹⁸ W. W. Jacobs,¹³ M. Janik,³⁹ I. Johnson,¹⁸ P. G. Jones,³ E. G. Judd,⁴ S. Kabana,⁴³ M. Kaneta,¹⁸ M. Kaplan,⁷ D. Keane,¹⁷ J. Kiryluk,⁶ A. Kisiel,³⁹ J. Klay,¹⁸ S. R. Klein,¹⁸ A. Klyachko,¹³ D. D. Koetke,³⁷ T. Kolleger,¹² A. S. Konstantinov,²⁷ M. Kopytine,¹⁷ L. Kotchenda,²¹ A. D. Kovalenko,¹⁰ M. Kramer,²² P. Kravtsov,²¹ K. Krueger,¹ C. Kuhn,¹⁵ A. I. Kulikov,¹⁰ A. Kumar,²⁵ G. J. Kunde,⁴³ C. L. Kunz,⁷ R. Kh. Kutuev,¹¹ A. A. Kuznetsov,¹⁰ M. A. C. Lamont,³ J. M. Landgraf,² S. Lange,¹² C. P. Lansdell,³⁶ B. Lasiuk,⁴³ F. Laue,² J. Lauret,² A. Lebedev,² R. Lednický,¹⁰ V. M. Leontiev,²⁷ M. J. LeVine,² C. Li,³² Q. Li,⁴¹ S. J. Lindenbaum,²² M. A. Lisa,²⁴ F. Liu,⁴² L. Liu,⁴² Z. Liu,⁴² Q. J. Liu,⁴⁰ T. Ljubicic,² W. J. Llope,³⁰ H. Long,⁶ R. S. Longacre,² M. Lopez-Noriega,²⁴ W. A. Love,² T. Ludlam,² D. Lynn,² J. Ma,⁶ Y. G. Ma,³³ D. Magestro,²⁴ S. Mahajan,¹⁶ L. K. Mangotra,¹⁶ D. P. Mahapatra,¹⁴ R. Majka,⁴³ R. Manweiler,³⁷ S. Margetis,¹⁷ C. Markert,⁴³ L. Martin,³⁴ J. Marx,¹⁸ H. S. Matis,¹⁸ Yu. A. Matulenko,²⁷ T. S. McShane,⁸ F. Meissner,¹⁸ Yu. Melnick,²⁷ A. Meschanin,²⁷ M. Messer,² M. L. Miller,⁴³ Z. Milosevich,⁷ N. G. Minaev,²⁷ C. Mironov,¹⁷ D. Mishra,¹⁴ J. Mitchell,³⁰ B. Mohanty,³⁸ L. Molnar,²⁸ C. F. Moore,³⁶ M. J. Mora-Corral,¹⁹ V. Morozov,¹⁸ M. M. de Moura,⁴¹ M. G. Munhoz,³¹ B. K. Nandi,³⁸ S. K. Nayak,¹⁶ T. K. Nayak,³⁸ J. M. Nelson,³ P. Nevski,² V. A. Nikitin,¹¹ L. V. Nogach,²⁷ B. Norman,¹⁷ S. B. Nurushev,¹⁷ G. Odyniec,¹⁸ A. Ogawa,² V. Okorokov,²¹ M. Oldenburg,¹⁸ D. Olson,¹⁸ G. Paic,²⁴ S. U. Pandey,⁴¹ S. K. Pal,³⁸ Y. Panebratsev,¹⁰ S. Y. Panitkin,² A. I. Pavlinov,⁴¹ T. Pawlak,³⁹ V. Perevoztchikov,² W. Peryt,³⁹ V. A. Petrov,¹¹ S. C. Phatak,¹⁴ R. Picha,⁵ M. Planinic,⁴⁴ J. Pluta,³⁹ N. Porile,²⁸ J. Porter,² A. M. Poskanzer,¹⁸ M. Potekhin,² E. Potrebenikova,¹⁰ B. V. K. S. Potukuchi,¹⁶ D. Prindle,⁴⁰ C. Pruneau,⁴¹ J. Putschke,¹⁹ G. Rai,¹⁸ G. Rakness,¹³ R. Raniwala,²⁹ S. Raniwala,²⁹ O. Ravel,³⁴ S. V. Razin,^{10,13} D. Reichhold,²⁸ J. G. Reid,⁴⁰ G. Renault,³⁴ F. Retiere,¹⁸ A. Ridiger,²¹ H. G. Ritter,¹⁸ J. B. Roberts,³⁰ O. V. Rogachevski,¹⁰ J. L. Romero,⁵ A. Rose,⁴¹ C. Roy,³⁴ L. J. Ruan,^{32,2} V. Rykov,⁴¹ R. Sahoo,¹⁴ I. Sakrejda,¹⁸ S. Salur,⁴³ J. Sandweiss,⁴³ I. Savin,¹¹ J. Schambach,³⁶ R. P. Scharenberg,²⁸ N. Schmitz,¹⁹ L. S. Schroeder,¹⁸ K. Schweda,¹⁸ J. Seger,⁸ D. Seliverstov,²¹ P. Seyboth,¹⁹ E. Shalahiev,¹⁰ M. Shao,³² M. Sharma,²⁵ K. E. Shestermanov,²⁷ S. S. Shimanskii,¹⁰ R. N. Singaraju,³⁸ F. Simon,¹⁹ G. Skoro,¹⁰ N. Smirnov,⁴³ R. Snellings,²³ G. Sood,²⁵ P. Sorensen,⁶ J. Sowinski,¹³ H. M. Spinka,¹ B. Srivastava,²⁸ S. Stanislaus,³⁷ R. Stock,¹² A. Stolpovsky,⁴¹ M. Strikhanov,²¹ B. Stringfellow,²⁸ C. Struck,¹² A. A. P. Suaide,⁴¹ E. Sugarbaker,²⁴ C. Suire,² M. Šumbera,⁹ B. Surrow,² T. J. M. Symons,¹⁸ A. Szanto de Toledo,³¹ P. Szarwas,³⁹ A. Tai,⁶ J. Takahashi,³¹ A. H. Tang,^{2,23} D. Thein,⁶ J. H. Thomas,¹⁸ V. Tikhomirov,²¹ M. Tokarev,¹⁰ M. B. Tonjes,²⁰ S. Trentalange,⁶ R. E. Tribble,³⁵ M. D. Trivedi,³⁸ V. Trofimov,²¹ O. Tsai,⁶ T. Ullrich,² D. G. Underwood,¹ G. Van Buren,² A. M. VanderMolen,²⁰ A. N. Vasiliev,²⁷ M. Vasiliev,³⁵ S. E. Vigdor,¹³ Y. P. Viyogi,³⁸ S. A. Voloshin,⁴¹ W. Waggoner,⁸ F. Wang,²⁸ G. Wang,¹⁷ X. L. Wang,³² Z. M. Wang,³² H. Ward,³⁶ J. W. Watson,¹⁷ R. Wells,²⁴ G. D. Westfall,²⁰ C. Whitten, Jr.,⁶ H. Wieman,¹⁸ R. Willson,²⁴ S. W. Wissink,¹³ R. Witt,⁴³ J. Wood,⁶ J. Wu,³² N. Xu,¹⁸ Z. Xu,² Z. Z. Xu,³² A. E. Yakutin,²⁷ E. Yamamoto,¹⁸ J. Yang,⁶ P. Yepes,³⁰ V. I. Yurevich,¹⁰ Y. V. Zanevski,¹⁰ I. Zborovský,⁹ H. Zhang,^{43,2} H. Y. Zhang,¹⁷ W. M. Zhang,¹⁷ Z. P. Zhang,³² P. A. Zolnierczuk,¹³ R. Zoulkarneev,¹¹ J. Zoulkarneeva,¹¹ and A. N. Zubarev¹⁰

(STAR Collaboration*)

¹Argonne National Laboratory, Argonne, Illinois 60439, USA²Brookhaven National Laboratory, Upton, New York 11973, USA³University of Birmingham, Birmingham, United Kingdom⁴University of California, Berkeley, California 94720, USA⁵University of California, Davis, California 95616, USA⁶University of California, Los Angeles, California 90095, USA⁷Carnegie Mellon University, Pittsburgh, Pennsylvania 15213, USA⁸Creighton University, Omaha, Nebraska 68178, USA⁹Nuclear Physics Institute AS CR, Rež/Prague, Czech Republic¹⁰Laboratory for High Energy (JINR), Dubna, Russia

- ¹¹Particle Physics Laboratory (JINR), Dubna, Russia
¹²University of Frankfurt, Frankfurt, Germany
¹³Indiana University, Bloomington, Indiana 47408, USA
¹⁴Institute of Physics, Bhubaneswar 751005, India
¹⁵Institut de Recherches Subatomiques, Strasbourg, France
¹⁶University of Jammu, Jammu 180001, India
¹⁷Kent State University, Kent, Ohio 44242, USA
¹⁸Lawrence Berkeley National Laboratory, Berkeley, California 94720, USA
¹⁹Max-Planck-Institut fuer Physik, Munich, Germany
²⁰Michigan State University, East Lansing, Michigan 48824, USA
²¹Moscow Engineering Physics Institute, Moscow Russia
²²City College of New York, New York City, New York 10031, USA
²³NIKHEF, Amsterdam, The Netherlands
²⁴Ohio State University, Columbus, Ohio 43210, USA
²⁵Panjab University, Chandigarh 160014, India
²⁶Pennsylvania State University, University Park, Pennsylvania 16802, USA
²⁷Institute of High Energy Physics, Protvino, Russia
²⁸Purdue University, West Lafayette, Indiana 47907, USA
²⁹University of Rajasthan, Jaipur 302004, India
³⁰Rice University, Houston, Texas 77251, USA
³¹Universidade de São Paulo, São Paulo, Brazil
³²University of Science and Technology of China, Anhui 230027, China
³³Shanghai Institute of Nuclear Research, Shanghai 201800, People's Republic of China
³⁴SUBATECH, Nantes, France
³⁵Texas A and M, College Station, Texas 77843, USA
³⁶University of Texas, Austin, Texas 78712, USA
³⁷Valparaiso University, Valparaiso, Indiana 46383, USA
³⁸Variable Energy Cyclotron Centre, Kolkata 700064, India
³⁹Warsaw University of Technology, Warsaw, Poland
⁴⁰University of Washington, Seattle, Washington 98195, USA
⁴¹Wayne State University, Detroit, Michigan 48201, USA
⁴²Institute of Particle Physics, CCNU (HZNU), Wuhan 430079, China
⁴³Yale University, New Haven, Connecticut 06520, USA
⁴⁴University of Zagreb, Zagreb HR-10002, Croatia
- (Received 8 July 2003; published 31 October 2003)

We present the results of charged particle fluctuations measurements in Au+Au collisions at $\sqrt{s_{NN}} = 130$ GeV using the STAR detector. Dynamical fluctuations measurements are presented for inclusive charged particle multiplicities as well as for identified charged pions, kaons, and protons. The net charge dynamical fluctuations are found to be large and negative providing clear evidence that positive and negative charged particle production is correlated within the pseudorapidity range investigated. Correlations are smaller than expected based on model-dependent predictions for a resonance gas or a quark-gluon gas which undergoes fast hadronization and freeze-out. Qualitative agreement is found with comparable scaled $p+p$ measurements and a heavy ion jet interaction generation model calculation based on independent particle collisions, although a small deviation from the $1/N$ scaling dependence expected from this model is observed.

DOI: 10.1103/PhysRevC.68.044905

PACS number(s): 25.75.Ld

A key question of the heavy ion program at the relativistic heavy ion collider (RHIC) is to understand whether the hot matter produced in the midst of heavy ion collisions undergoes a transition to and from a quark-gluon plasma (QGP) phase before it hadronizes. One of the most striking signatures of such a QGP-HG (hadron gas) phase transition could be a strong modification in the fluctuations of specific ob-

servables measured on a per collision basis, i.e., event by event [1–4]. Most often discussed are mean transverse momentum fluctuations (temperature fluctuations) and particle multiplicity fluctuations. For the latter, predictions range from enhanced multiplicity fluctuations connected to the production of QGP droplets and nucleation processes in a first order QGP-HG phase transition, to a strong suppression of fluctuations as a consequence of rapid freeze-out just after the phase transition [4,5]. In this case, final state values of conserved quantities, such as net electric charge, baryon

*URL: www.star.bnl.gov

number, and strangeness would not be strongly modified from their values in the QGP stage. Due to the large difference in the degrees of freedom in the QGP and HG phases, measured fluctuations, of the net electric charge, in particular, could be reduced by a factor ranging from 2 to 4 if a QGP is produced [4,5]. The frequency of production and size of QGP droplets may critically depend on the collision impact parameter. Central collisions are generally expected to lead to larger and more frequent QGP droplet production. An increase in the size and production frequency of QGP droplets with increasing collision centrality might then be signaled by a sudden change in the fluctuations of produced particles such as antiprotons and kaons [6], as well as pions.

In this paper, we report on a measurement of charged particle multiplicity fluctuations as a function of collision centrality in Au+Au collisions at an energy of $\sqrt{s_{NN}} = 130$ GeV. We study event-by-event fluctuations of conserved quantities at near-zero rapidity in the center-of-mass rest frame (midrapidity). Specifically, we discuss fluctuations in the difference of the number of produced positively and negatively charged particles (multiplicities) measured in a fixed rapidity range, defined as [7]

$$\nu_{+-} = \left\langle \left(\frac{N_+}{\langle N_+ \rangle} - \frac{N_-}{\langle N_- \rangle} \right)^2 \right\rangle, \quad (1)$$

where N_+ and N_- are multiplicities of positive and negative particles calculated in a specific pseudorapidity, and transverse momentum range. The notation “ $\langle O \rangle$ ” denotes an average of the quantity O over an ensemble of events. The method used to calculate the averages $\langle N_+ \rangle$ and $\langle N_- \rangle$, which vary with collision centrality, is described in the following [see Eqs. (6)–(10)]. We consider fluctuations in the production of all charged particles, N_+ and N_- (mostly pions), as well as specific cases of proton and antiproton, N_p and $N_{\bar{p}}$, and positive and negative kaons, N_{K^+} and N_{K^-} , fluctuations. The former amounts to a measurement of net electrical charge fluctuations, whereas the latter corresponds to measurements of net baryon number and net strangeness fluctuations. The method used to calculate this and other observables used in this work is described in the following.

A difficulty inherent in the interpretation of measurements of multiplicity fluctuations is the elimination of effects associated with uncertainties in the collision centrality, often referred to as volume fluctuations. Event-by-event impact parameter variations, in particular, induce positive correlations in particle production which do not depend on the intrinsic dynamical properties of the colliding system, but rather simply reflect changes in the number of collision participants. Fluctuations in the difference of relative multiplicities ν_{+-} defined in Eq. (1), are however free from this problem. This analysis is thus restricted to the study of such relative multiplicities. As shown in Ref. [7], ν_{+-} can be readily translated into observables D , and ω_Q , discussed by other authors [4–6]. Its relation to the two-particle density is discussed below. We will additionally study the behavior of relative multiplicities ν_{+-} and other quantities of interest defined in this paper as a function of the collision centrality estimated

on the basis of the total charged particle multiplicity measured in the pseudorapidity range $|\eta| < 0.75$ in order to identify possible changes in the fluctuations with collision centrality.

The magnitude of the variance, ν_{+-} , is determined by both statistical and dynamical fluctuations. Statistical fluctuations arise due to the finite number of particles measured, and can be readily calculated based on expectation values for Poisson distributions as follows:

$$\nu_{+-,stat} = \frac{1}{\langle N_+ \rangle} + \frac{1}{\langle N_- \rangle}. \quad (2)$$

The statistical fluctuations depend on the experimental efficiency and analysis cuts used in the reconstruction of charged particle trajectories (tracks). The intrinsic or dynamical fluctuations are defined and evaluated as the difference between the measured fluctuations and the statistical limit

$$\nu_{+-,dyn} = \nu_{+-} - \nu_{+-,stat}. \quad (3)$$

As shown in Ref. [7], the dynamical fluctuations $\nu_{+-,dyn}$ can be expressed as follows:

$$\nu_{+-,dyn} = \bar{R}_{++} + \bar{R}_{--} - 2\bar{R}_{+-}, \quad (4)$$

where \bar{R}_{ab} with $a, b = +, -$ are the averages of the correlation functions often used in multiparticle production analysis [8–10]:

$$\bar{R}_{ab} = \frac{\int_{\Delta\eta} R_{2,ab}(\eta_a, \eta_b) \rho_{1,a}(\eta_a) \rho_{1,b}(\eta_b) d\eta_a d\eta_b}{\int_{\Delta\eta} \rho_{1,a}(\eta_a) d\eta_a \int_{\Delta\eta} \rho_{1,b}(\eta_b) d\eta_b}, \quad (5)$$

where $R_{2,ab} = \rho_2(\eta_a, \eta_b) / [\rho_{1,a}(\eta_a) \rho_{1,b}(\eta_b)] - 1$, $\rho_1(\eta) = dn/d\eta$, and $\rho_2(\eta_a, \eta_b) = d^2n/d\eta_a d\eta_b$ are single- and two-particle pseudorapidity densities, respectively. The integrals could most generally be taken over the full particle phase space (d^3p) but are here restricted (without loss of generality) to pseudorapidity integrals to simplify the notation. In cases where the produced particles are totally uncorrelated, two-particle densities can be factorized as products of two single-particle densities. The correlators \bar{R}_{ab} shall then vanish, and the measured dynamical fluctuations $\nu_{+-,dyn}$ should be identically zero. A deviation from zero thus should indicate correlations in particle production. If correlations are due to production via many subcollisions, localized sources, or clusters, one should further expect the strength of the correlation to be finite but increasingly diluted with increased number of production clusters or subcollisions (hereafter called “clusters”). The correlators \bar{R}_{ab} will be inversely proportional to the multiplicity of clusters, and thus also inversely proportional to the total measured multiplicity of (charged) particles [7]. Measurements at the ISR and FNAL, have shown that charged particles have long range (differential) correlations dominated by a dependence on the relative rapidity of the cor-

related particles. One thus expects, as shown in Ref. [7], that the functions \bar{R}_{ab} and $\nu_{+,-,dyn}$ should vary slowly with the detector acceptance as long as the rapidity width of the acceptance is smaller or of the order of the long range correlation width. This should however be experimentally verified by varying the acceptance used in the determination of $\nu_{+,-,dyn}$.

Authors [11,12] have suggested that if the reaction dynamics do not change with collision centrality, the measure $\Phi \approx \langle N_{ch} \rangle \nu_{dyn} / 8$ (where N_{ch} is the charged particle multiplicity in the rapidity range considered) should be independent of the collision centrality. Conversely, a significant collision centrality dependence of Φ or related observables should hint at a change in the collision dynamics. We shall thus study the collision centrality dependence of both $\nu_{+,-,dyn}$ and $\langle N_{ch} \rangle \nu_{+,-,dyn}$. The correlators \bar{R}_{ab} and $\nu_{+,-,dyn}$ are robust variables: their measurements are independent of the average (global) detection efficiencies involved in the determination of multiplicities N_+ and N_- [7]. The measurement of $\nu_{+,-,dyn}$ thus does not require explicit efficiency corrections. Second order corrections are, in principle, needed to account for variations of the detection efficiency through the fiducial acceptance. In the present study, we verified that the relative variation of the detection efficiency (about 10% in the transverse momentum region under study) results in a systematic uncertainty less than or equal to the statistical error of the measured values.

The data presented are from minimum bias and central trigger samples of Au+Au at $\sqrt{s_{NN}}=130$ GeV acquired by the STAR experiment during the first operation of the relativistic heavy ion collider (summer 2000). Detailed descriptions of the experiment and the time projection chamber (TPC) can be found elsewhere [13]. In minimum-bias mode, events were triggered by a coincidence between the two zero degree calorimeters located ± 18 m from the interaction center and a minimum signal in the central trigger barrel (CTB), which consists of scintillator slats surrounding the TPC. The central trigger sample was acquired by requiring a higher multiplicity cut with the CTB corresponding to 15% of the total hadronic cross section.

In order to minimize the need for corrections to account for dependence of the detector acceptance and reconstruction efficiency on the vertex position, the analysis reported here was restricted to events produced within ± 0.70 m of the center of the STAR TPC along the beam axis. In this range, the vertex finding efficiency is 100% for collisions which result in charged particle multiplicities larger than 50 tracks in the TPC acceptance. It decreases to 60% for events with fewer than five tracks from the primary vertex. We verified that the measurement of $\nu_{+,-,dyn}$ is insensitive to the vertex position by comparing values measured for different vertex cut ranges. About 180 000 minimum bias and 80 000 central trigger events were used in this analysis after cuts.

The centrality of the collisions is estimated from the total charged particle track multiplicity detected within the TPC in the pseudorapidity range $|\eta| < 0.75$. We use eight contiguous centrality bins based on the fraction of triggered events: 6%, 11%, 18%, 26%, 34%, 45%, 58%, and 84%. The trigger

efficiency is estimated to $94 \pm 2\%$. The above fractions thus correspond to a constant increase in the fraction of the geometrical cross section which is sampled by each multiplicity bin.

Particle production is studied for both negative and positive hadrons over a transverse momentum range extending from 0.1 to 5 GeV/c, and for pseudorapidity ranges from $|\eta| \leq 0.1$ to 1.0 in steps of 0.1 unit of pseudorapidity. Good track quality is required by restricting the analysis to charge particle tracks producing more than 15 hits within the TPC. One additionally requires that more than 50% of the hits be included in the final fit of the track.

One uses the particle energy loss dE/dx measured with the TPC to identify the particles as pions, kaons, and protons (and their antiparticles). Particle identification proceeds on the basis of a parametrization of the mean $\langle E_{loss} \rangle$ and width σ of the average energy loss expected for electrons, pions, kaons, and protons as a function of their momentum. The analyses for pions, kaons, and protons are performed using momentum ranges $0.1 < p < 0.6$, $0.15 < p < 0.6$, and $0.25 < p < 0.7$ GeV/c, respectively. Lower bounds are set near or below detection threshold to maximize particle yields. Upper bounds are used to minimize cross species contamination. The inclusive analysis of all charged species is performed within the range $0.1 < p < 5.0$ GeV/c. Limiting the particle momenta for this analysis to less than 5 GeV/c insured that particle charge was not misassigned while allowing for a fully inclusive measurement of the soft particle spectra. Given that the bulk of the particle production is below 2 GeV/c, the inclusive analysis is rather insensitive to the exact value of the upper bound which is used. The detection efficiency rises from zero to roughly 85% within an interval of 0.1 GeV/c above detection thresholds, remaining constant for larger momenta. Measured particles are tagged as pions if their measured energy loss deviates by less than two standard deviations (2σ) from the expected mean for pions of the same momentum, while deviating by more than 2σ for kaons of that same momentum. Similarly particles are identified as kaons (protons) if the deviation from the kaon (proton) mean energy is less than 2σ while being larger than 2σ from the pion and proton (kaon) mean energy loss. Contamination of the kaons and protons by pions is negligible at low momentum, and estimated to be less than 5% at the highest momenta accepted for those particles. For cross-species contamination at this level, it was verified that the measurement is insensitive to the actual value of the momentum cuts.

To reduce contamination from secondary electron tracks, and focus this analysis on primary tracks, i.e., particles produced at the Au+Au collision vertex, only tracks which passed within 3 cm of the collision vertex were accepted. We verified electron (positron) contamination has a negligible impact on our measurements of $\nu_{+,-,dyn}$ by repeating the analysis with and without an electron/positron exclusion cut based on the track energy loss measured in the TPC, i.e., accepting tracks with a dE/dx more than two standard deviations away from the expected value for an electron of the measured momentum.

As already mentioned, the measurement of $\nu_{+-,dyn}$ is independent of the average detector efficiency. It is therefore also insensitive to particle losses, e.g., antiprotons, due to scattering through the detector. It is however sensitive, in principle, to the generation of background particles within the detector. The effect of such background particles (e.g., protons scattered off the beam pipe) is minimized by using the 3 cm distance of closest approach cut mentioned above. Also, it was considered whether finite track splitting, possibly encountered in the reconstruction of charged particle tracks in the TPC, may produce measurable effects on $\nu_{+-,dyn}$. We verified that, within statistical errors, the same value is obtained when the pseudorapidity regions used to count positive and negative tracks were separated by a $\Delta\eta=0.25$ gap.

Since finite width multiplicity bins were used for this analysis, values of $\nu_{+-,dyn}$ are multiplicity-bin averaged according to the following expression:

$$\nu_{+-,dyn}(M_{low} \leq M < M_{high}) = \frac{\sum \nu_{+-,dyn}(M)P(M)}{\sum P(M)}, \quad (6)$$

where $P(M)$ is the probability of having a total charge multiplicity M and $\nu_{+-,dyn}(M)$ is given by

$$\nu_{+-,dyn}(M) = \frac{\langle N_+(N_+ - 1) \rangle_M}{\langle N_+ \rangle_M^2} + \frac{\langle N_-(N_- - 1) \rangle_M}{\langle N_- \rangle_M^2} - 2 \frac{\langle N_+ N_- \rangle_M}{\langle N_+ \rangle_M \langle N_- \rangle_M}. \quad (7)$$

The notation $\langle O \rangle_M$ is used to indicate the average of the quantity O for all events with a charged particle multiplicity M in the pseudorapidity range $|\eta| < 0.75$. Our analysis proceeds in two passes. The first pass involves the determination of the averages $\langle N_{\pm} \rangle_M$ as a function of the multiplicity M using unity bin width in M while the second pass uses these averages as coefficients in the above expression of $\nu_{+-,dyn}(M)$. The averages $\langle N_{\pm} \rangle_M$ are determined from the events with multiplicity M :

$$\langle N_{\pm} \rangle_M = \frac{1}{N_{ev}(M)} \sum N_{\pm}. \quad (8)$$

The sum is taken over the $N_{ev}(M)$ events of multiplicity M present in our sample. The averages $\langle N_{\pm} \rangle_M$ thus obtained display a scatter determined by the finite statistics about a monotonically increasing trend (with M). If uncorrected, this scatter, may induce an artificial change of the value of $\nu_{+-,dyn}(M)$ in each bin. To minimize this effect, we model (fit) the average $\langle N_{\pm} \rangle_M$ dependence on the multiplicity M with a polynomial optimized to reproduce the shape of the dependence. We then determine $\nu_{+-,dyn}(M)$ using the averages $\langle N_{\pm} \rangle_{fit,M} \equiv \bar{N}_{\pm,M}$ predicted by the fit rather than the actual averages. The calculation of $\nu_{+-,dyn}$ in a finite width multiplicity bin then proceeds with the following expression:

$$\begin{aligned} & \nu_{+-,dyn}(M_{low} \leq M < M_{high}) \\ &= \frac{1}{N_{ev \text{ events}}} \sum \left[\frac{N_+(N_+ - 1)}{\bar{N}_{+,M}^2} + \frac{N_-(N_- - 1)}{\bar{N}_{-,M}^2} - 2 \frac{N_+ N_-}{\bar{N}_{+,M} \bar{N}_{-,M}} \right], \end{aligned} \quad (9)$$

where the sum is taken over the N_{ev} events in the multiplicity bin $M_{low} \leq M < M_{high}$.

The quantity $\langle N \rangle \nu_{+-,dyn}$ is determined in a similar fashion using the following expression:

$$\begin{aligned} & \langle N \rangle \nu_{+-,dyn}(M_{low} \leq M < M_{high}) \\ &= \frac{1}{N_{ev \text{ events}}} \sum (\bar{N}_{+,M} + \bar{N}_{-,M}) \left[\frac{N_+(N_+ - 1)}{\bar{N}_{+,M}^2} + \frac{N_-(N_- - 1)}{\bar{N}_{-,M}^2} \right. \\ & \quad \left. - 2 \frac{N_+ N_-}{\bar{N}_{+,M} \bar{N}_{-,M}} \right]. \end{aligned} \quad (10)$$

To study the effect of this method of bin averaging, a simulation was performed using HIJING (heavy ion jet interaction generator) events, comparing the results of Eqs. (10) and (3) in the limit of large statistics. The HIJING model does not incorporate rescattering and should not therefore exhibit a significant centrality dependence. The results showed that for all bins except the lowest multiplicity bin used for this analysis, the two equations gave the same result within the quoted systematics. In the first multiplicity bin, Eq. (10) yielded a result $\approx 15\%$ larger than Eq. (3).

Figure 1(a) shows the dynamical fluctuations $\nu_{+-,dyn}$ of the net charge measured in the pseudorapidity range $|\eta| \leq 0.5$, as a function of the total multiplicity M measured in the pseudorapidity range $|\eta| \leq 0.75$. The horizontal bars on the data points reflect the width of the multiplicity bins used in this analysis while the vertical bars reflect statistical errors. We estimate the systematic errors based on data taken and analyzed with different trigger and analysis cuts, to be of the order of 2%. An additional systematic uncertainty of the order of 3% is derived by a separate analysis of different data subsets. The dynamical fluctuations of the 5% most central collisions then amount to $\nu_{+-,dyn} = -0.00236 \pm 0.00006(\text{stat}) \pm 0.00012(\text{syst})$. The dynamical fluctuations are finite and negative: a clear indication that positive and negative particle production are correlated within the pseudorapidity range considered [see Eq. (4)]. One observes the strength of the dynamical fluctuations decreases monotonically with increasing collision centrality. This can be understood from the fact that more central Au+Au collisions involve an increasing number of ‘‘subcollisions’’ (e.g., nucleon-nucleon collisions): the two-particle correlations are thus increasingly diluted and the magnitude of $\nu_{+-,dyn}$ is effectively reduced.

We compare our results, for the most central collisions, to those recently reported by the PHENIX Collaboration [14] which measured net charge fluctuations in terms of the relative variance $\omega_Q = \langle \Delta Q^2 \rangle / N_{ch}$ in the rapidity range $|\eta| < 0.35$, and the angular range $\Delta\Phi = \pi/2$, for $p_{\perp} > 200$ MeV/c. They reported a value $\omega_Q = 0.965 \pm 0.007(\text{stat}) - 0.019(\text{syst})$ for the 10% most central collisions. The (unidirectional) systematic

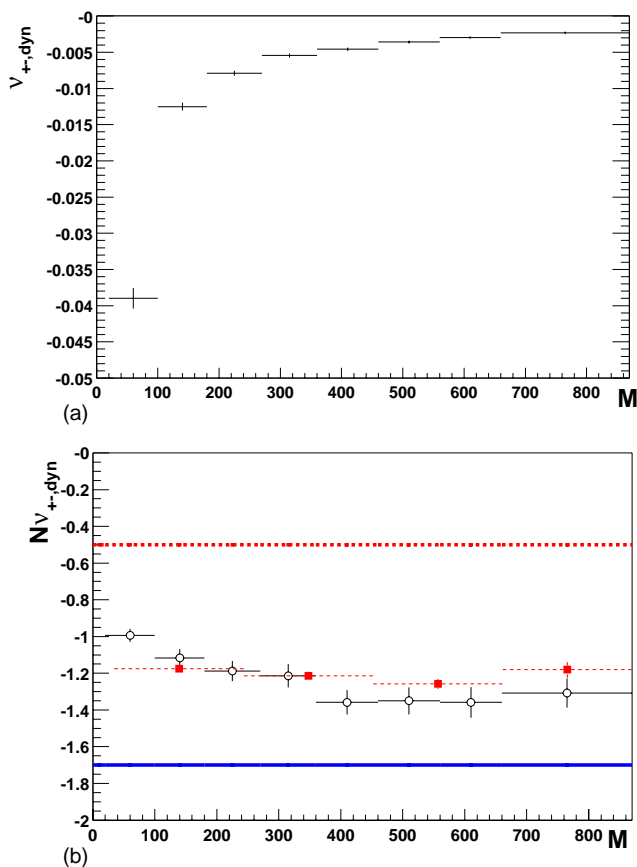


FIG. 1. (Color online) (a) Dynamical fluctuations $\nu_{+-,dyn}$ measured in $|\eta| \leq 0.5$ as a function of the collision centrality estimated with the total (uncorrected) multiplicity M in $|\eta| < 0.75$. Error shown are statistical only. Systematic error estimated to 5%. (b) $\langle N \rangle \nu_{+-,dyn}$ measured in $|\eta| \leq 0.5$ vs M (opened circles) compared to the charge conservation limit (dotted line), resonance gas expectation based on Ref. [5] (solid line), and HIJING calculation (solid squares). Errors shown are statistical only. Systematic error estimated to 10%.

error is reported to correspond to the net effects of detector inefficiencies and background tracks not assigned the correct charge. In order to compare the PHENIX result with the present study, we use the expression in Ref. [7]

$$\nu_{+-,dyn} = \frac{4}{N_+ + N_-} (\omega_Q - 1). \quad (11)$$

The charged particle multiplicity in the PHENIX detector acceptance is 79 ± 5 for the 10% most central collisions. This comparison gives $\nu_{+-,dyn} = -0.0018 \pm 0.0004(\text{stat}) - 0.0009(\text{syst})$ in agreement with the value of $\nu_{+-,dyn} = -0.00263 \pm 0.00009(\text{stat}) \pm 0.00012(\text{syst})$ we measure for 11% central collisions. The agreement is best if one considers the low bound of the PHENIX measurement which is maximally corrected for finite efficiency (which is reflected in the systematic error). The difference between the two results might be due, in part, to dependence of the multiplicity fluctuations on rapidity and azimuthal angle as well as acceptance effects.

It is important to consider the effects of charge conservation on the net charge fluctuations since they are expected to be non-negligible even for small finite rapidity coverage [7]. The contribution is estimated to be $-4/\langle N \rangle_{4\pi}$ where $\langle N \rangle_{4\pi}$ is the total number of charged particles produced by the collisions. The PHOBOS Collaboration has reported [15] that the total charged particle multiplicity amounts to 4200 ± 470 in the 6% most central Au+Au collisions at $\sqrt{s_{NN}} = 130$ GeV. The charge conservation contribution to the measured dynamical fluctuations is thus of the order of -0.00095 ± 0.0001 , i.e., 40% of the observed dynamical fluctuations.

We next discuss the centrality dependence of the fluctuations. In central collisions, the measured dynamical fluctuations $\nu_{+-,dyn}$ are expected to be reduced due to dilution of the two-particle correlations. One expects the magnitude of $\nu_{+-,dyn}$ should scale inversely to the number of subcollisions producing particles. Assuming the average number of particles produced by such subcollisions is independent of the collision centrality, one then expects the fluctuations to scale inversely as the charged particle multiplicity. The quantity $\langle N \rangle \nu_{+-,dyn}$ should therefore be independent of collision centrality if no significant variation in the mechanism of the particle production arises with collision centrality. This notion was suggested by Gazdzicki [12] and Mrowczynski [11] in terms of the fluctuation measure Φ which, as shown in Ref. [7], is equal to $\langle N \rangle \nu_{+-,dyn} / 8$ for $\langle N_+ \rangle \approx \langle N_- \rangle$. Figure 1(b) shows the measured centrality dependence of $\langle N \rangle \nu_{+-,dyn}$, calculated with Eq. (10), for all charged particles produced in the pseudorapidity range $|\eta| \leq 0.5$. In this figure, the charged particle multiplicity N is corrected for finite detection efficiencies using correction factors which depend linearly on the charged particle multiplicity (TPC detector occupancy) with values ranging from 85% to 70% for peripheral and central collisions, respectively [16]. The measured values range from -1 to -1.4 and are approximately a factor of 2 larger than the charge conservation limit, shown as a dotted line, in Fig. 1(b). This indicates dynamical fluctuations are not only finite but in fact rather large. As discussed in detail below, the values measured for $\langle N \rangle \nu_{+-,dyn}$ however fall short of predictions for a resonance gas in equilibrium (≈ -1.7 ; solid line) and for a scenario involving a quark-gluon gas undergoing fast hadronization [≈ -3.5 ; not shown in Fig. 1(b)] [5]. The measured values are in qualitative agreement with a calculation based on HIJING (solid squares) [17]. Indeed, the values predicted by HIJING are within 20% of the measured values at all centralities. While the HIJING calculation is independent of collision centrality, the experimental data exhibit a small but finite centrality dependence which is significant above the first bin in Fig. 1(b). The HIJING calculation does not feature rescattering, and is therefore not expected to exhibit a significant centrality dependence. The observed centrality dependence may then suggest there are rescattering effects, or other dynamical effects with centrality, and its interpretation requires further investigation.

The magnitude of the net charge dynamical fluctuations is determined by the strength of the two-particle correlations in the integrated rapidity range. Measurements from $p+p$ colli-

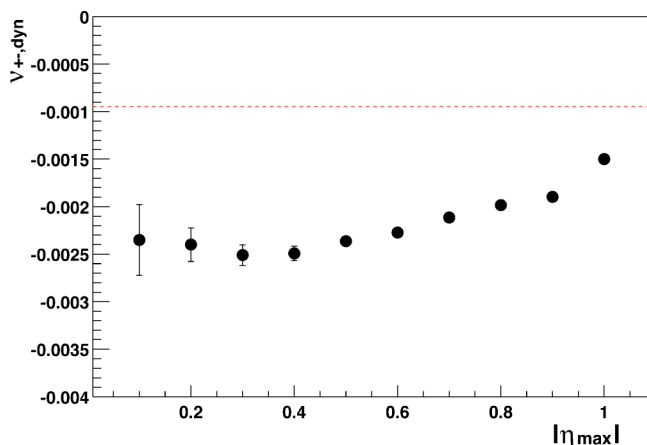


FIG. 2. (Color online) Fluctuations $\nu_{+-,dyn}$ for the 6% most central collisions as a function of the range of integrated pseudorapidities. Errors shown are statistical only. Systematic errors are estimated to range from 5% at $|\eta|>0.4$ to 20% at $|\eta|=0.1$. The expected limit due to charge conservation is shown as a dotted line.

sions at the ISR and $p+\bar{p}$ collisions at FNAL indicate that the relevant rapidity interval for two-particle correlations is approximately one unit. One thus expects the dynamical fluctuations to exhibit a mild dependence on the rapidity range used for the measurement [7]. Figure 2 shows the measured dynamical fluctuations (filled circles) as a function of the pseudorapidity range. The pseudorapidity integration range is varied from $-0.1 < \eta < 0.1$ to $-1.0 < \eta < 1.0$ in discrete steps of 0.1 units of pseudorapidity. Error bars shown are statistical only. Focusing on the region in Fig. 2 where systematic effects due to finite multiplicities are expected to be small, we examine the data for $|\eta|>0.4$. One observes the absolute value of the dynamical fluctuations is largest in this range for $|\eta|\approx 0.4$, and that it decreases monotonically for larger acceptance without, however, reaching the charge conservation limit. One finds $|\nu_{dyn}|$ decreases by 35%–40% while the integrated pseudorapidity range is increased by a factor of 5 from 0.4 to 2 pseudorapidity units. The dependence of dynamical fluctuations on the experimental acceptance is rather modest. In contrast, the Φ measure increases approximately by a factor of 10 from $-0.1 < \eta < 0.1$ to $-1.0 < \eta < 1.0$ due to its explicit dependence on the pseudorapidity bin size.

We next consider the above results in the light of correlation functions measured in $p+p$ and $p+\bar{p}$ collisions at CERN and FNAL [18,19,8] with the use of Eq. (4). To account for the unavailability of $p+p$ comparison data at the same energy as RHIC, an interpolation was made using results obtained at lower and higher collision energies (parametrization from Ref. [20]). Based on results published in Refs. [18,19,8], we also note that the correlation function for oppositely charged particles, $R_{+}(y_{+}\approx y_{-})$, is found to be approximately twice as strong as the same sign particles correlations, $R_{++}\approx R_{--}$ [8,9], and that it is independent of the collision energy. The CERN and FNAL measurements [18,19,8] find the single charged particle and two-particle (charged-charged) pseudorapidity densities to be, respectively, $\rho_1(\eta=0)\approx 2.06$ and $C_2(0,0)=\rho_2(\eta_1=0,\eta_2=0)-\rho_1(\eta_1=0)\rho_1(\eta_2=0)\approx 2.8$. The charged-

charged correlation integral $R_{cc}=(R_{++}+R_{--}+2R_{+-})/4$ is thus $R_{cc}\approx 0.66$ (see Ref. [7]). Furthermore, assuming equal multiplicities of positively and negatively charged particles, one finds for the charged-charged correlation $R_{cc}\approx 1.5R_{++}$, which we use to estimate the correlation measured in this work as $\bar{R}_{++}+\bar{R}_{--}-2\bar{R}_{+-}\approx -2\bar{R}_{++}\approx 4\bar{R}_{cc}/3\approx 0.88$. The pseudorapidity densities are very different in $p+p$ and $A+A$ collisions. Under assumption that the correlations are due to production in a finite number of sources (clusters), they should be inversely proportional to the particle density. In the 5% most central Au+Au collisions, the pseudorapidity charged particle density ($dN/d\eta$) is about $526\pm 2(\text{stat})\pm 36(\text{syst})$ [16] compared to ≈ 2.06 in $p\bar{p}$ collisions. Such a dilution would give for the correlation function a value of $0.88\times 2.06/526\approx 0.0034$, in qualitative agreement with the measured values for Au+Au collisions presented in this paper. We stress that valuable insight can be gained by comparing the current 130-GeV data and upcoming 200-GeV Au+Au analysis with explicit measurements made in $p+p$ collisions rather than using the above first order approximation.

We next compare our measurement of the dynamical fluctuations to predictions of net charge fluctuations based on thermal models [4,5,21–23]. To this end, we express our measurement of $\nu_{+-,dyn}$ in the range $|\eta|\leq 0.5$ in terms of the D variable introduced in Ref. [5], using

$$D = 4 + \langle N \rangle \nu_{+-,dyn} \quad (12)$$

valid for $N_{+}\approx N_{-}$ [7]. We find using data shown in Fig. 1(b) that D decreases from 3.1 ± 0.05 (statistical error only) for the most peripheral collisions measured to 2.8 ± 0.05 in central collisions. However, a comparison to thermal model predictions requires the data to be corrected for charge conservation effects. One must subtract the charge conservation contribution which amounts to $\Delta D = -0.00095 \times 526 = -0.50\pm 0.06$. The corrected values of D thus range from 3.6 ± 0.1 to 3.2 ± 0.1 . According to the discussion of Refs. [4,5,21–23], these values approach that ($D\approx 2.8$) expected for a resonance gas. They are significantly larger than expected in the above referenced work [21,5,23,22] for a quark-gluon gas undergoing fast hadronization and freeze-out ($D\approx 1$). It is not possible to draw a firm conclusion concerning the existence or non-existence of a deconfined phase during the collisions from these results since, as the above authors have pointed out, incomplete thermalization could lead to larger fluctuations than expected for a QGP. Other work [24] has also suggested that the prediction of $D\approx 1$ for a quark-gluon gas is model dependent, and that other effects such as gluon fragmentation prior to hadronization could increase the fluctuations expected even if a quark-gluon plasma were produced.

We extend the study of net charge fluctuations to identified particles and consider measurements of the net charge fluctuations of pions, kaons, and protons/antiprotons. Measurement of the K^{+}, K^{-} and p, \bar{p} net charge are of particular interest as they address, respectively, fluctuations of net strangeness and baryon number which might be more sensitive to the details of the collision process. The results are

TABLE I. $1000\nu_{+-,dyn}$ for charged pions, kaons, and protons, as a function of the integrated pseudorapidity range. Errors shown are statistical only. Systematic errors are estimated to be of the order of 10% for charged pions and kaons, and of the order of 20% for protons and antiprotons.

$ \eta $	All $+-$	π^\pm	K^\pm	p, \bar{p}
0.5	-2.36 ± 0.06	-2.4 ± 0.1	-5 ± 3	-3 ± 7
0.6	-2.27 ± 0.04	-2.4 ± 0.1	-5 ± 2	-5 ± 3
0.7	-2.11 ± 0.04	-2.18 ± 0.08	-4 ± 2	-7 ± 5
0.8	-1.98 ± 0.03	-2.12 ± 0.07	-6 ± 2	-8 ± 3
0.9	-1.90 ± 0.03	-2.02 ± 0.06	-6 ± 2	-9 ± 2
1.0	-1.75 ± 0.02	-1.92 ± 0.06	-7 ± 1	-8 ± 2

compiled in Table I for all charged species, pions, kaons, and p, \bar{p} . The results indicate that the dynamical fluctuations for pions are approximately of the same magnitude as for inclusive nonidentified charged particles. One however discerns a small but finite difference, especially for integrated pseudorapidity ranges $|\eta| \leq 0.7$ and larger. The measurement of K^+, K^- and p, \bar{p} fluctuations is hampered by the smaller multiplicities and finite detection efficiencies for kaons and protons and their antiparticles. Our measurement, which is presented in Table I for acceptances from $|\eta| \leq 0.5$ to $|\eta| \leq 1.0$ is thus limited to a central collision trigger sample. The effect of the variation of efficiency near detection threshold was studied by changing the transverse momentum threshold used in the determination of $\nu_{+-,dyn}$. It was found that for inclusive nonidentified particles, $\nu_{+-,dyn}$ changed by less than 3% while varying the transverse momentum cutoff for particle detection from 0.1 to 0.2 GeV/c. The same study using HIJING events led to a 10% change in $\nu_{+-,dyn}$.

The systematic error for protons (antiprotons) is difficult to assess, since GEANT studies indicate a considerable fraction of the proton yield below 0.4 GeV/c is associated with pion-induced proton knockout reactions in the beam pipe. Background protons bear little correlation with antiprotons. The terms R_{++} and R_{+-} involved in the calculation of $\nu_{+-,dyn}$ should have a Poissonian behavior, and therefore the contribution of uncorrelated background to these terms should partly cancel. We find the value of $\nu_{+-,dyn}$ exhibit changes smaller than the statistical uncertainties when raising the threshold from 0.2 to 0.3 GeV/c, and hence ascribe a systematic error of the order of 20% for the p, \bar{p} measurement.

The dynamical fluctuations of the charged kaons and p, \bar{p} are also finite. Their size (absolute value) are in fact larger than the dynamical fluctuations measured for pions and for inclusive nonidentified charged particles. The proton dynamical fluctuations are somewhat larger than the kaon fluctuations. Strangeness conservation and baryon number conservation should influence the size of the dynamical fluctuations for the net charge of kaons and p, \bar{p} , respectively. The charge conservation limit derived for inclusive nonidentified charged particles can be readily reinterpreted to estimate the expected magnitude of dynamical fluctuations for K^+, K^- and p, \bar{p} . One finds that the kaon and p, \bar{p} dynamical fluctuations are similar or slightly larger than their respective charge conservation limits.

We have measured event-by-event net charge dynamical fluctuations for inclusive nonidentified charged particles, as well as for identified pions, kaons, and protons and their antiparticles in Au+Au collisions at $\sqrt{s_{NN}}=130$ GeV. Dynamical fluctuations measured for inclusive nonidentified charged particles are finite and exceed by nearly a factor of 2 expectations based on charge conservation. We find the magnitude of the net charge dynamical fluctuations to be in qualitative agreement with expectations based on measurements of charged particle correlation functions in $p+p$ collisions measured at the ISR. We however find that although the fluctuations roughly scale in proportion to the reciprocal of the produced charged particle multiplicity, the scaling is not perfect, and the quantity $\langle N \rangle \nu_{+-,dyn}$ exhibits a small dependence on collision centrality, which suggests the two-particle correlations may be modified in central collisions relative to peripheral collisions.

A comparison of our measurement with thermal model predictions [21,5,22] appear to indicate fluctuations at a level that might be expected if the Au+Au system behaved like a resonance gas. Although the size of the fluctuations is significantly larger than expected in that work for a quark-gluon gas, limitations of the model used prevent a conclusion on the existence or nonexistence of a quark-gluon plasma phase based on these results.

Finally, we report the first measurement of net charge dynamical fluctuations of identified pions, kaons, and protons. Pions exhibit dynamical fluctuations slightly larger than the values obtained with our inclusive measurement. Kaons and protons are found to exhibit dynamical fluctuations that are 2 to 4 times larger than those observed for all charged particles. However, the lower production multiplicities of these particles may imply the dynamical fluctuations are dominated by charge conservation effects. Further data are needed to assess whether the dynamical fluctuations of kaons (protons) significantly exceed the minimal values constrained by strangeness (baryon) charge conservation.

We wish to thank the RHIC Operations Group and the RHIC Computing Facility at Brookhaven National Laboratory, and the National Energy Research Scientific Computing Center at Lawrence Berkeley National Laboratory for their support. This work was supported by the Division of Nuclear Physics and the Division of High Energy Physics of the Office of Science of the U.S. Department of Energy, the United States National Science Foundation, the Bundesministerium fuer Bildung und Forschung of Germany, the Institut National de la Physique Nucleaire et de la Physique des Particules of France, the United Kingdom Engineering and Physical Sciences Research Council, Fundacao de Amparo a Pesquisa do Estado de Sao Paulo, Brazil, the Russian Ministry of Science and Technology, the Ministry of Education of China, the National Natural Science Foundation of China, Stichting voor Fundamenteel Onderzoek der Materie, the Grant Agency of the Czech Republic, Department of Atomic Energy of India, Department of Science and Technology of India, Council of Scientific and Industrial Research of the Government of India, and the Swiss National Science Foundation.

- [1] E. V. Shuryak, Phys. Lett. B **423**, 9 (1998).
[2] K. Rajagopal, Nucl. Phys. **A661**, 150c (1999).
[3] L. Stodolsky, Phys. Rev. Lett. **75**, 1044 (1995).
[4] M. Asakawa, U. Heinz, and B. Mueller, Phys. Rev. Lett. **85**, 2072 (2000).
[5] S. Jeon and V. Koch, Phys. Rev. Lett. **85**, 2076 (2000).
[6] S. Gavin and C. Pruneau, Phys. Rev. C **61**, 044901 (2000).
[7] C. Pruneau, S. Gavin, and S. Voloshin, Phys. Rev. C **66**, 044904 (2002).
[8] L. Foa, Phys. Rep., Phys. Lett. **22**, 1 (1975).
[9] J. Whitmore, Phys. Rep., Phys. Lett. **27**, 187 (1976).
[10] H. Boggild and T. Ferbel, Annu. Rev. Nucl. Sci. **24**, 451 (1974).
[11] S. Mrowczynski, Phys. Rev. C **66**, 024904 (2002).
[12] M. Gazdzicki, Eur. Phys. J. C **8**, 131 (1999).
[13] K. H. Ackermann *et al.*, STAR Collaboration, Nucl. Phys. **A661**, 681c (1999).
[14] K. Adcox *et al.*, PHENIX Collaboration, Phys. Rev. Lett. **89**, 082301 (2002); J. Nystrand (private communication).
[15] B. Back *et al.*, PHOBOS Collaboration, Phys. Rev. Lett. **87**, 102303 (2001).
[16] C. Adler *et al.*, STAR Collaboration, Phys. Rev. Lett. **87**, 112303 (2001).
[17] X. N. Wang and M. Gyulassy, Phys. Rev. D **44**, 3501 (1991).
[18] R. E. Ansorge *et al.*, UA5 Collaboration, Z. Phys. C: Part. Fields **37**, 191 (1988).
[19] S. R. Amendolia *et al.*, Nuovo Cimento Soc. Ital. Fis., A **31A**, 17 (1976).
[20] G. J. Alner *et al.*, UA5 Collaboration, Z. Phys. C: Part. Fields **33**, 1 (1986).
[21] S. Jeon and V. Koch, Phys. Rev. Lett. **83**, 5435 (1999).
[22] V. Koch, M. Bleicher, and S. Jeon, Nucl. Phys. **A698**, 261 (2002).
[23] M. Bleicher, S. Jeon, and V. Koch, Phys. Rev. C **62**, 061902 (2000).
[24] S. J. Lindenbaum and R. S. Longacre, nucl-th/0108061.